QSAR-QMMM Cryptographic Mining on Chern-Simons Topological Geometrics for the generation of a Ligand Targeting COVID-19-SARS-COV-2 SPIKE D614G Binding Sites.

Ioannis Grigoriadis[1]

[1]Biogenea Pharmaceuticals Ltd

April 05, 2024

Abstract

SARS coronavirus 2 (SARS-CoV-2) in the viral spike (S) encoding a SARS-COV-2 SPIKE D614G mutation protein predominate over time in locales revealing the dynamic aspects of its key viral processes where it is found, implying that this change enhances viral transmission. It has also been observed that retroviruses infected ACE2-expressing cells pseudotyped with SG614 that is presently affecting a growing number of countries markedly more efficiently than those with SD614. In this paper, we strongly combine topology geometric methods targeting at the atomistic level the protein apparatus of the SARS-COV-2 virus that are simple in machine learning anti-viral characteristics, to propose computer-aided rational drug design strategies efficient in computing docking usage, and powerful enough to achieve very high accuracy levels for this in-silico effort for the generation of the AI-Quantum designed molecule of Combination of GisitorviffirnaTM, Roccustyrna_gs1_TM, and Roccustyrna_fr1_TM ligands with Preferred IUPAC Names of (7aR)-5-amino-N-[(S)-{2-[(S)-[(E)-(amino methyl idene)amino](cyano)methyl]hydrazin-1-yl}(aziridin-1-yl)phosphoryl]-1-[(2E)-2-[(fluoromethanimidoyl)imino]acetyl]-7-oxo-1H,7H,7aH-pyrazolo[4,3-d]pyrimidine-3-carboxamide; N-{[(2-amino- 6-oxo-6,9-dihydro-1H-purin-9-yl)amino]({1-[5- ({[cyano({1-[(diaminomethylidene)amino]ethenyl})amino]oxy}methyl)-3,4-dihydroxyoxolan-2-yl]-1H-1,2,4-triazol-3-yl}formamido)phosphoryl}-6-fluoro-3,4-dihydropyrazine-2-carboxamide;[3-(2-amino-5-sulfanylidene-1,2,4-triazolidin-3-yl)oxaziridin-2-yl]({3-sulfanylidene-1,2,4,6-tetraazabicyclo[3.1.0]hexan-6-yl})phosphoroso1-(3,4,5-trifluorooxolan-2-yl)-1H-1,2,4-triazole-3-carboxylate targeting the COVID-19-SARS-COV-2 SPIKE D614G mutation using Chern-Simons Topology Euclidean Geometric in a Lindenbaum-Tarski generated QSAR automating modeling and Artificial Intelligence-Driven Predictive Neural Networks.

Hosted file

`RoccustyrnaiJN_qqchCcamOmgt7HK__ Grigoriadis_Ioannis_.doc` available at https://authorea.com/users/389434/articles/709336-qsar-qmmm-cryptographic-mining-on-chern-simons-topological-geometrics-for-the-generation-of-a-ligand-targeting-covid-19-sars-cov-2-spike-d614g-binding-sites

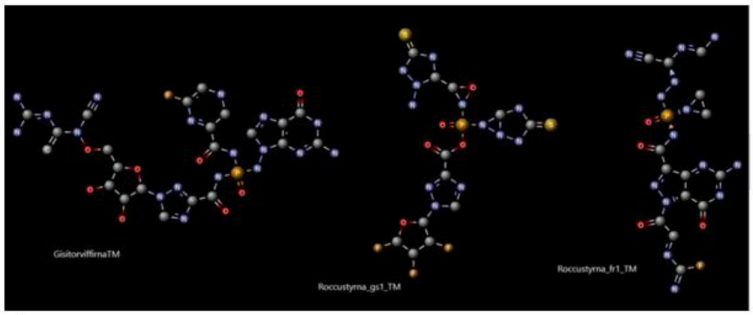

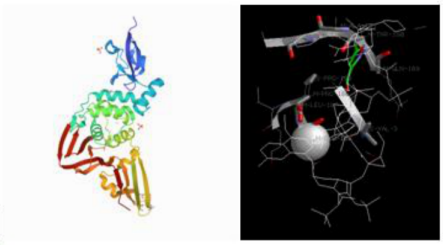

3D Docking Interactions of the combination of GisitorviffirnaTM, Roccustyrna_gs1_TM, and Roccustyrna_fr1_TM fragments 2D structure inside the PDB: 6WZU protein targets of the crystal structures of Papain-Like Protease of SARS CoV-2, P3221 space group

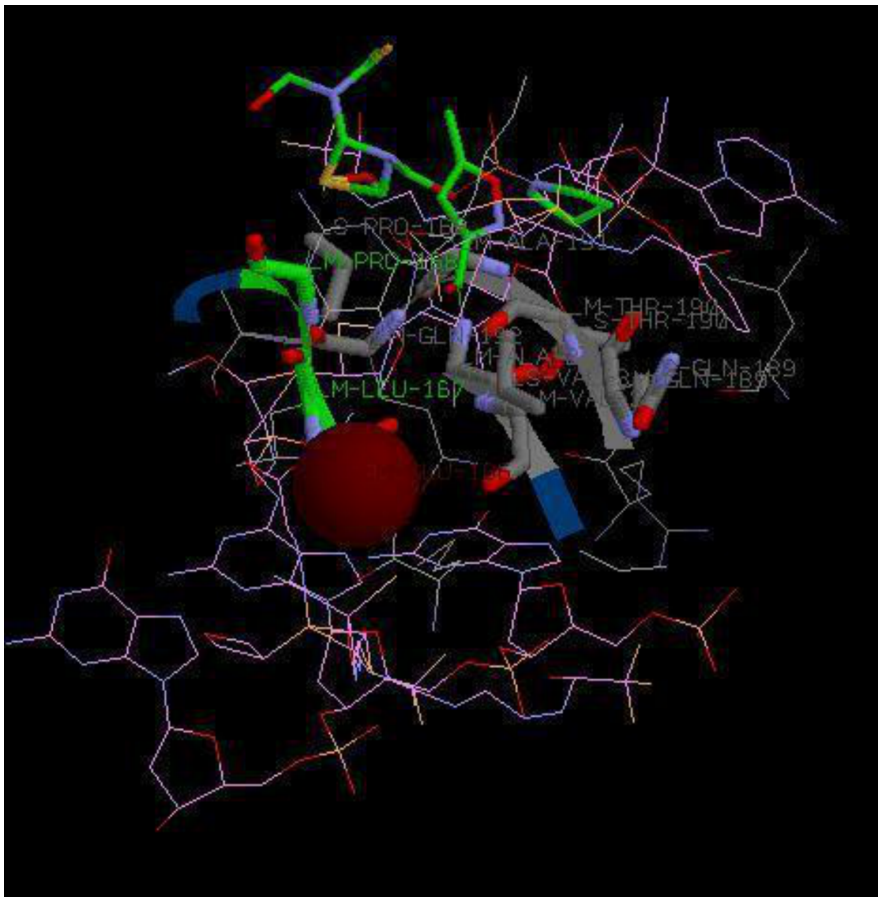

Hosted file

scheme_3..tiff available at https://authorea.com/users/389434/articles/709336-qsar-qmmm-cryptographic-mining-on-chern-simons-topological-geometrics-for-the-generation-of-a-ligand-targeting-covid-19-sars-cov-2-spike-d614g-binding-sites

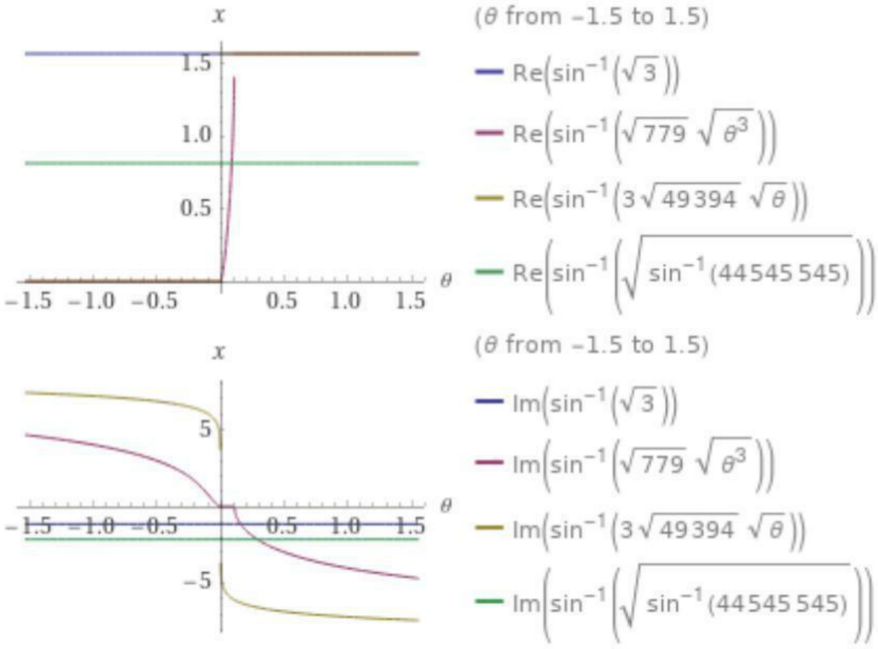

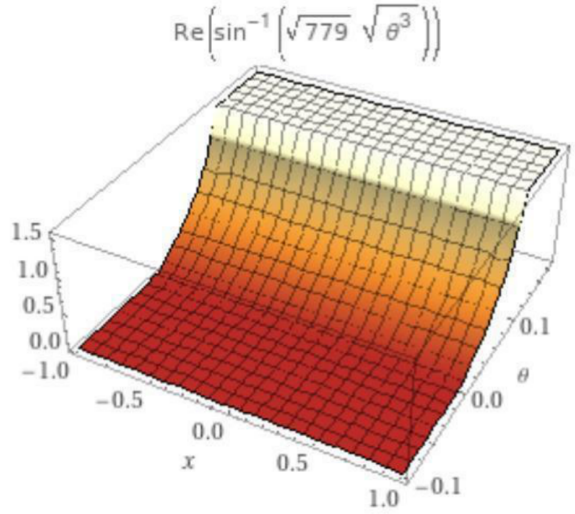

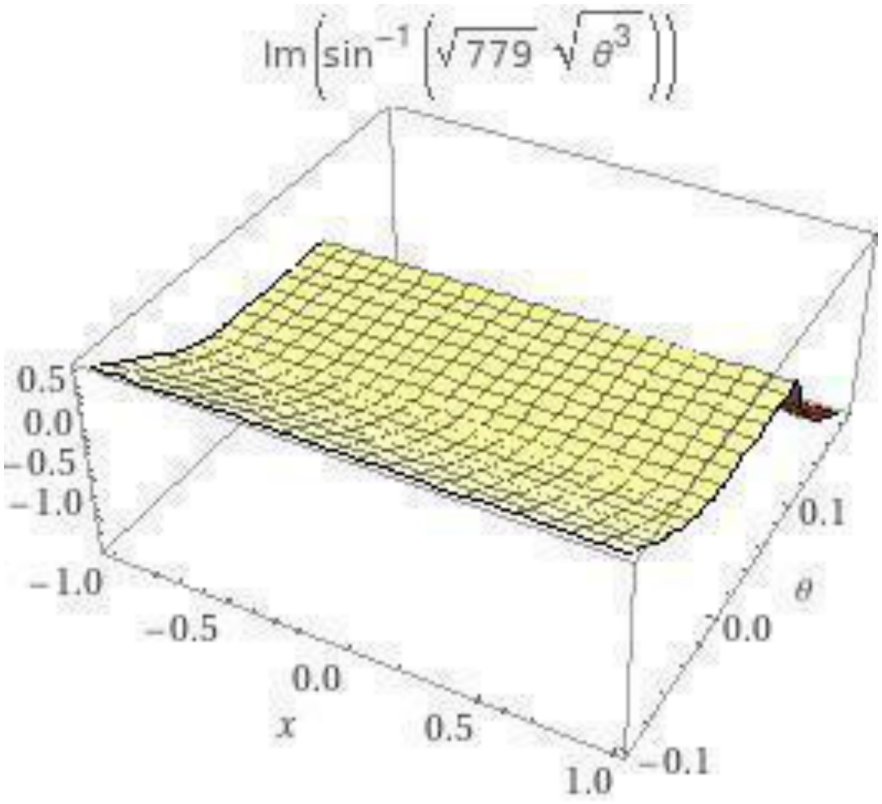

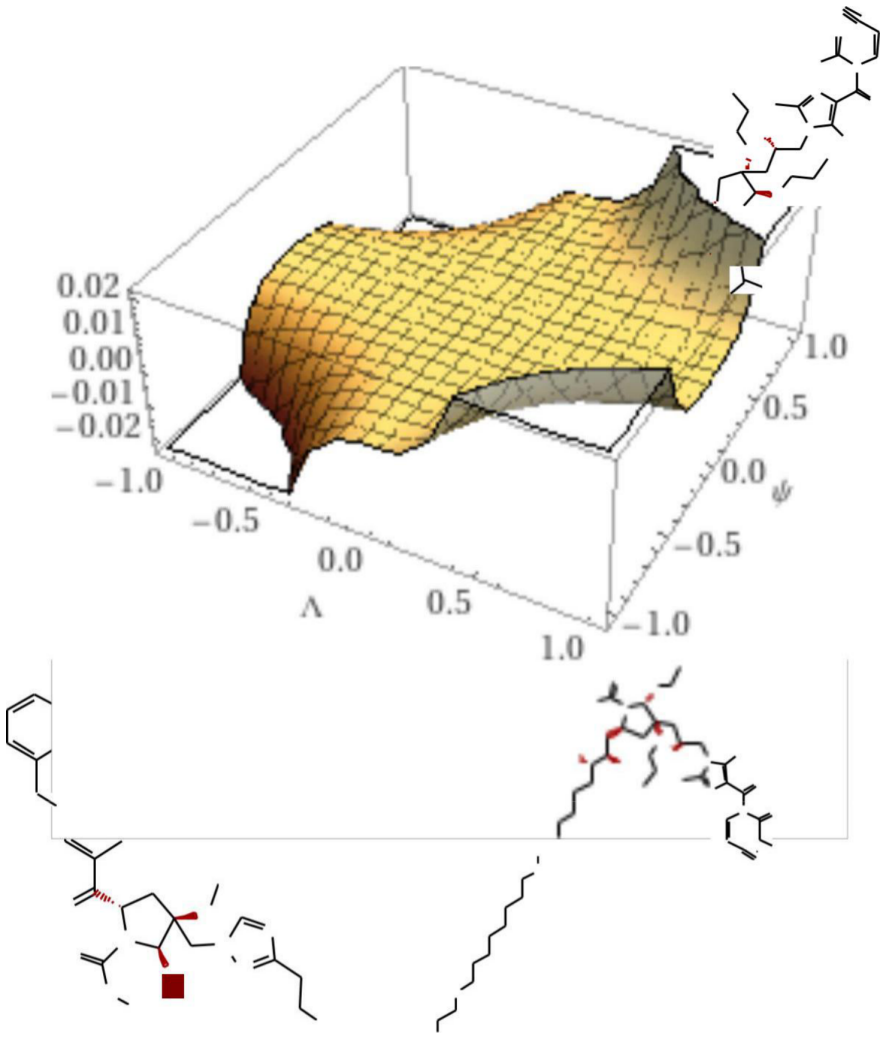

$$
\begin{aligned}
&-\log\left(\sqrt{1+14\,692\,375\,882\,461\,045\,811\,756\,348\,944\left(e^{-i\,X}-e^{i\,X}\right)^2 x(\tau)^2}-\right.\\
&\qquad\left.121\,212\,111\,121\,212\left(e^{-i\,X}-e^{i\,X}\right)x(\tau)\right)\\
&\log\left(\sqrt{\left(\left(1+x(\tau)^2 x'(22\,\tau)^{488}\log^2\left(\sqrt{\left(1-\frac{1}{4\,y(\tau)}x'(\right.\right.\right.\right.\\
&\qquad 22)^{576\,431\,275\,750\,959\,675\,405\,783\,039\,290\,773\,810\,744\,762\,062\,805\,850\,371\,259\,715\,614\,902\,742\,679\,552}\\
&\qquad\left.\left.\left.\left.\right)+\frac{1}{2\sqrt{y(\tau)}}i\,x'(\right.\right.\right.\right.\\
&\qquad\left.\left.\left.\left. 22)^{288\,215\,637\,875\,479\,837\,702\,891\,519\,645\,386\,905\,372\,381\,031\,402\,925\,185\,629\,857\,807\,451\,371\,339\,776}\right)y'(\right.\right.\right.\\
&\qquad\left.\left.\left.\tau)^{-2\,i\log\left(\sqrt{1+14\,692\,375\,882\,461\,045\,811\,756\,348\,944\left(e^{-i\,X}-e^{i\,X}\right)^2 x(\tau)^{44}}-121\,212\,111\,121\,212\left(e^{-i\,X}-e^{i\,X}\right)x(\tau)^{22}\right)}\right)\right.\\
&\qquad\left.+x(\tau)\,x'(22\,\tau)^{244}\log\left(\sqrt{\left(1-\frac{1}{4\,y(\tau)}x'(\right.\right.\right.\\
&\qquad 22)^{576\,431\,275\,750\,959\,675\,405\,783\,039\,290\,773\,810\,744\,762\,062\,805\,850\,371\,259\,715\,614\,902\,742\,679\,552}\\
&\qquad\left.\left.\left.\right)+\frac{1}{2\sqrt{y(\tau)}}i\,x'(\right.\right.\right.\\
&\qquad\left.\left. 22)^{288\,215\,637\,875\,479\,837\,702\,891\,519\,645\,386\,905\,372\,381\,031\,402\,925\,185\,629\,857\,807\,451\,371\,339\,776}\right)y'(\right.\right.\\
&\qquad\left.\left.\tau)^{-i\log\left(\sqrt{1+14\,692\,375\,882\,461\,045\,811\,756\,348\,944\left(e^{-i\,X}-e^{i\,X}\right)^2 x(\tau)^{44}}-121\,212\,111\,121\,212\left(e^{-i\,X}-e^{i\,X}\right)x(\tau)^{22}\right)}\right)\right.\\
&\qquad\left.\right)
\end{aligned}
$$

$$\left.\right) =$$

$$\frac{7}{3\,835\,k^4\,n^{33\,835}\,N^2\log(k) - 33\,834)}$$

$$334\,432$$

∞

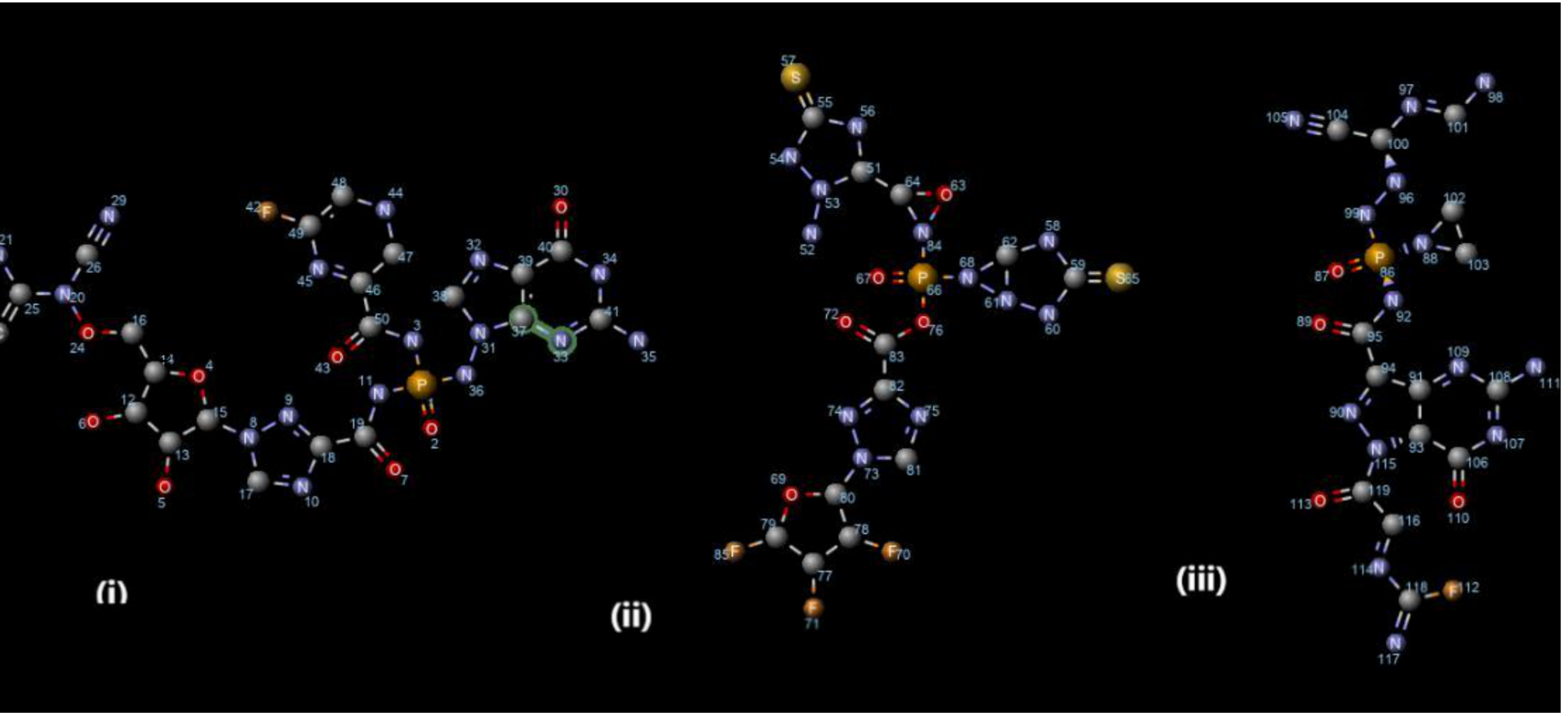

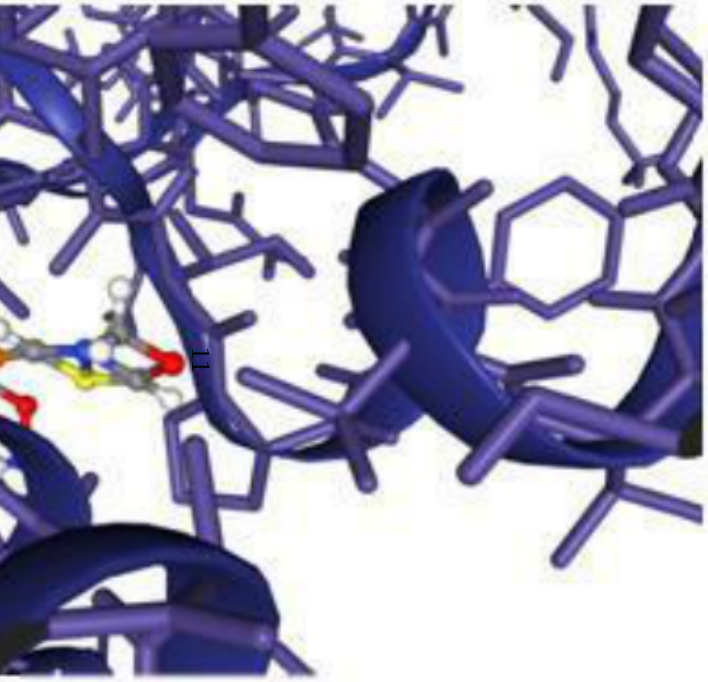

Figure2d

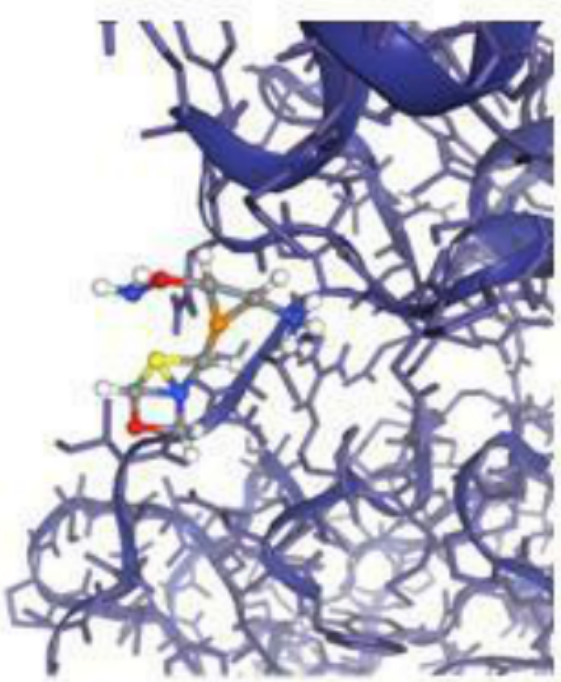

Figure2e

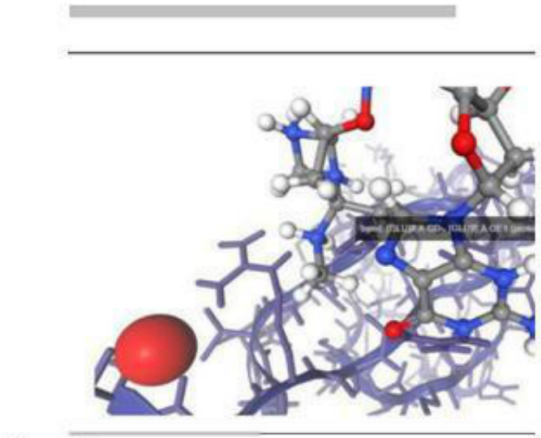

Figure3a

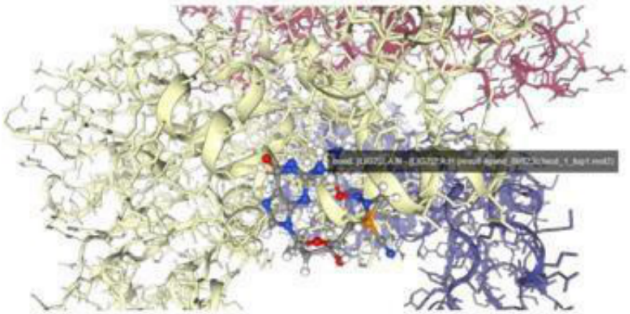

Figure3b

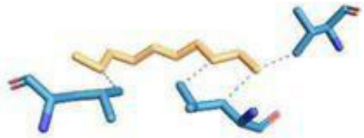

Figure3c

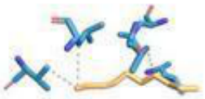

Figure3d

Figure3e

Figure3f

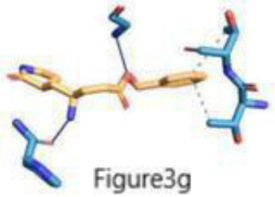

Figure3g

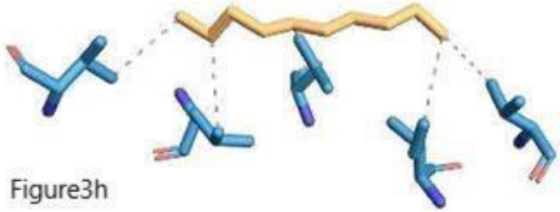

Figure3h

Figure4d

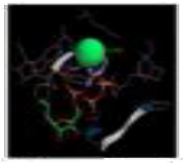

Figure4e

Figure4f

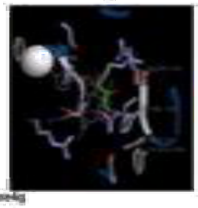

Figure4g

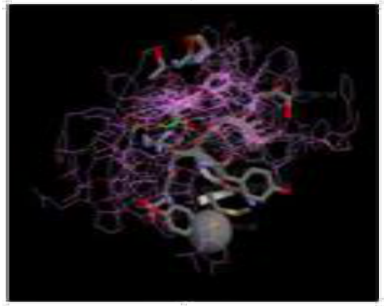

Figure4a

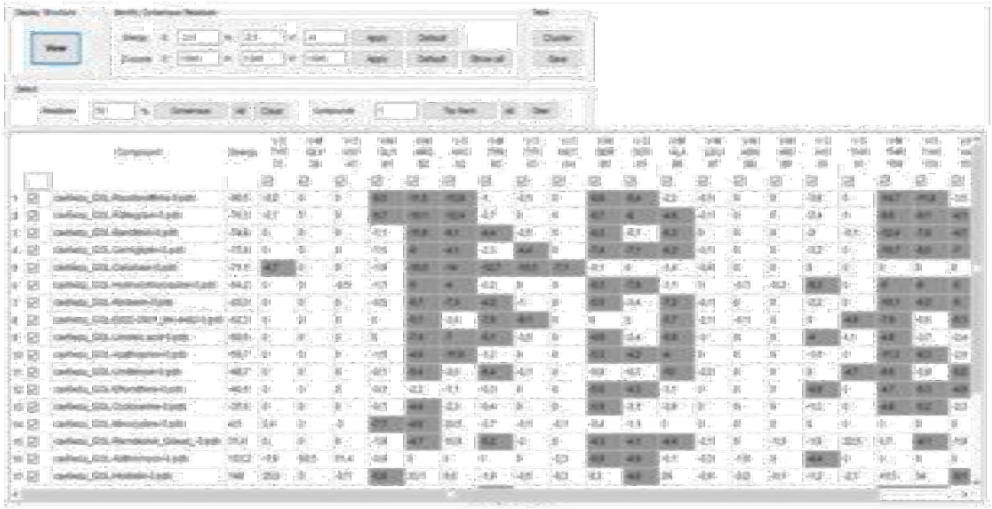

Figure4h

Predicted Low Energy MsMs Spectrum (10V), [M+H]+

Predicted Medium Energy MsMs Spectrum (2

Predicted High Energy MsMs Spectrum (40V), [M+H]+

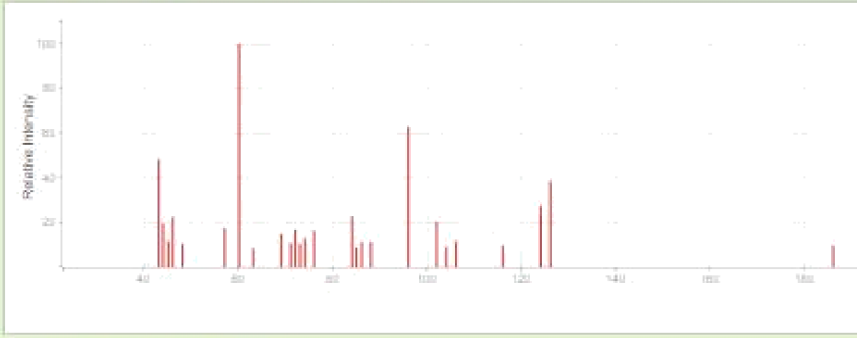

Peak Table and Fragment Structures

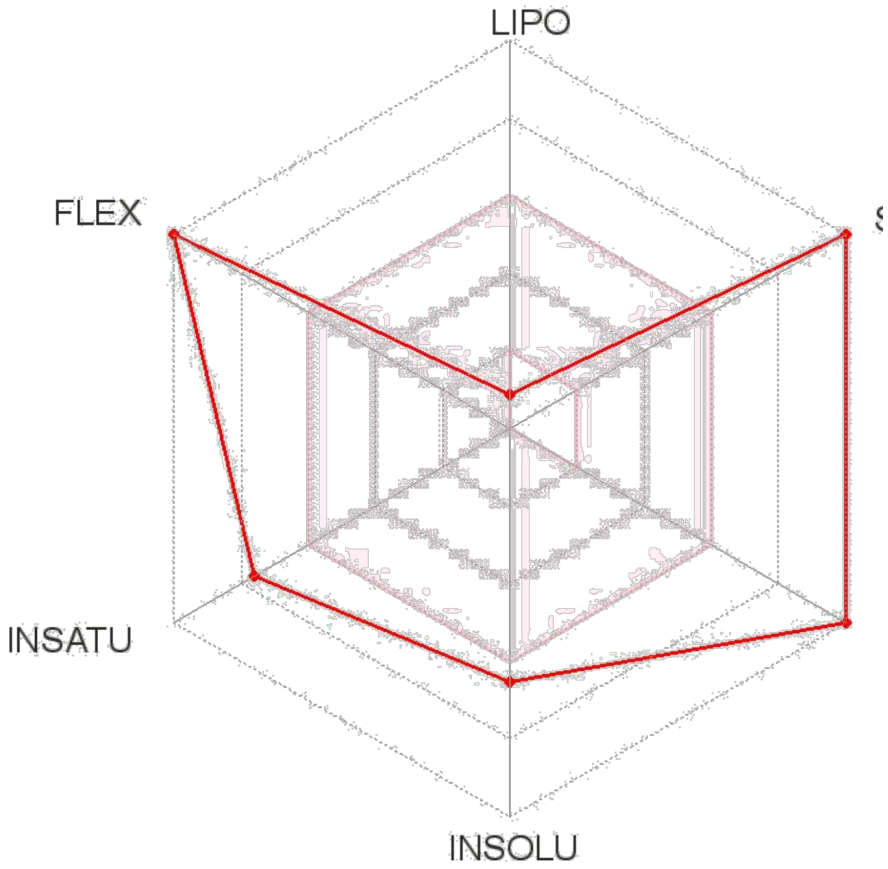

Hosted file

Table1_RoccustyrnaJGVY_.docx available at https://authorea.com/users/389434/articles/709336-qsar-qmmm-cryptographic-mining-on-chern-simons-topological-geometrics-for-the-generation-of-a-ligand-targeting-covid-19-sars-cov-2-spike-d614g-binding-sites

Hosted file

Table2._RoccustyrnaGFJ_.docx available at https://authorea.com/users/389434/articles/709336-qsar-qmmm-cryptographic-mining-on-chern-simons-topological-geometrics-for-the-generation-of-a-ligand-targeting-covid-19-sars-cov-2-spike-d614g-binding-sites

Hosted file

Table3._RoccustyrnaJVK_.docx available at https://authorea.com/users/389434/articles/709336-qsar-qmmm-cryptographic-mining-on-chern-simons-topological-geometrics-for-the-generation-of-a-ligand-targeting-covid-19-sars-cov-2-spike-d614g-binding-sites

Hosted file

Table4._RoccustyrnaJFD.-.docx available at https://authorea.com/users/389434/articles/709336-qsar-qmmm-cryptographic-mining-on-chern-simons-topological-geometrics-for-the-generation-of-a-ligand-targeting-covid-19-sars-cov-2-spike-d614g-binding-sites

Hosted file

Table5._RoccustyrnaJVN._.docx available at https://authorea.com/users/389434/articles/

709336-qsar-qmmm-cryptographic-mining-on-chern-simons-topological-geometrics-for-the-generation-of-a-ligand-targeting-covid-19-sars-cov-2-spike-d614g-binding-sites